Characteristics of "Monday Morning" Base Iron

Cathrine Hartung
Foundry Innovation – Elkem Silicon Products (ESP), Kristiansand, Norway

Leander Michels
Foundry Innovation – Elkem Silicon Products (ESP), Kristiansand, Norway
Department of Physics, Norwegian University of Science and Technology (NTNU), Trondheim, Norway

Bente Kroka
Elkem Technology, Kristiansand, Norway

Robert Schmidt
Grede St.Cloud, St.Cloud, Minnesota, USA

Mike Riabov, David Kesse
Elkem Materials, Inc., Pittsburgh, Pennsylvania, USA

ABSTRACT

The term "Monday morning" iron refers to metal that has been held in a furnace over an extended period, typically over a weekend. A key characteristic of these irons is their poor potential for graphite nucleation, often accompanied by a high amount of undercooled graphite. Foundries face a labor-intensive process to enhance the quality of this metal before casting. The undesirable microstructure is commonly attributed to the loss of carbon, that is, a change in the melt's chemistry. In this context, the current study examines the role of microinclusions in Monday morning irons under three conditions: after a prolonged holding time, following the addition of new carbon, and when the metal is ready for production use. The findings reveal that the poor nucleation condition is not due to carbon loss, but rather to a lower number density of microinclusions, especially sulfides. Additionally, there is a notable change in sulfide morphology, with the particles in the ready iron being rounder.

Keywords: cast iron, Monday morning iron, microinclusions, base iron

INTRODUCTION

The nucleation potential is the ability of a melt to form graphite. This is often measured in terms of low eutectic temperature[1] and the graphite morphology. In this context, the so called "Monday morning" irons represent one of the worst examples of a melt with a low nucleation potential. These types of melts are observed in a foundry's first batch of production after a long period of holding. They are undesirable because of their inconsistent quality and a high probability of forming defects.[2]

During solidification, graphite will nucleate on existing microinclusions dispersed in the melt. Inoculation is a way to increase the amount of nucleation sites, since the graphite morphology and number density of inclusions are substantially improved.[3,4] The effect of holding time on loss of nucleation potential has been systematically reported in the literature[5,6] and several reasons has been proposed, such as the Ostwald ripening, chemistry change, and loss of inclusions. Ostwald ripening states that smaller particles will dissolve, and larger particles will grow due to a concentration difference promoted by the difference in size. Chemistry change has mainly been associated with the loss of carbon, i.e., reduction of the carbon equivalent, due to longer holding times at high temperatures.[7] And loss of microinclusions reported as the case of reduction of nucleation sites, like Ostwald ripening, due to a reduction in the microinclusions number density.[8]

In lamellar graphite irons (grey iron), it is known that graphite flakes nucleate mainly on sulfides (MnS), which nucleate on Al-based oxides.[9] Riposan et al.[10] showed that inoculation mainly modifies the morphology of these (Mn,X)S compounds (where X = Fe, Al, Ca, Sr), causing them to change shape based on X addition. It has been reported that for X = Ca, the sulfide has an ovoid shape, while for X = Sr the sulfide has a regular polygonal shape. Therefore, a way to quantify the quality of a grey iron melt could be by evaluating the morphology of these Mn-

sulfides microinclusions. Rounder sulfides have been associated with better flake graphite structures and a lower eutectic undercooling.

In this context, a study of "Monday morning" iron is effectively a study of the base melt that solidifies as grey iron and has been on an extended holding time. The present investigation characterizes a holding furnace iron into three conditions: (i) after holding in 30 MT for an extended holding period, (ii) after being partly refreshed with 15 MT of newly melted high carbon iron, and (iii) after a further 15 MT addition of newly melted iron. This is done in terms of microstructure and microinclusion analyses, which is not often reported in grey iron research.

DESIGN OF EXPERIMENTS

SAMPLE DESCRIPTION

For this study, a base melt intended for ductile iron production was collected from a holding furnace. The samples are described in Table 1.

Table 1. Sample Description

Sample ID	Description
Sample 0 - SP0	"Monday Morning" iron collected/held over weekend just before new iron introduction.
Sample 1 - SP1	Collected after a 50% refresh of the bath with high carbon iron (3.87% C prior to tapping adjusted with petcoke derived recarburiser).
Sample 2 - SP2	Collected after 100% refresh of the holder with iron ready for production use.

CHEMICAL COMPOSITION

The composition of the samples is shown in Table 2.

Table 2. Chemical Composition of Samples

Elements	SP0	SP1	SP2
C	3.46	3.58	3.54
Si	2.12	2.12	2.13
Mg	-	-	0.0005
Mn	0.422	0.41	0.407
P	0.019	0.02	0.019
S	0.011	0.011	0.010
Cr	0.041	0.041	0.041
Al	0.002	0.002	0.003
Cu	0.156	0.165	0.151
Ti	0.008	0.008	0.008
V	0.006	0.006	0.007
Nb	0.008	0.008	0.008

All the samples contain similar levels of Si, Mn and S. Therefore, the main difference is the carbon content. Sample SP0 has the lowest, which is expected from a "Monday morning" iron, and SP1 has a higher carbon level due to the addition of recarburizer at the melting furnace.

AUTOMATED MINERAL IDENTIFICATION AND CHARACTERIZATION SYSTEM (AMICS)

After the microstructure quantification, the specimens were evaluated using scanning electron microscopy (SEM) equipped with the AMICS software. A Zeiss Merlin Compact SEM equipped with a Bruker XFlash 6130 energy-dispersive X-ray (EDX) detector was used combined with a backscattered electron (BSE) detector signal for the determination of chemical composition, phase composition, and particle size distribution. The minimum particle area measured was 0.5 μm^2. Below this value, the particle size and composition uncertainty are large and therefore not reported. The total evaluated area was 15.34 mm^2 (1520 fields at 1000x) for all samples.

RESULTS

THERMAL ANALYSIS

The cooling curves for all samples were collected using standard thermal analysis (TA) cups, which are small sand crucibles (36 × 36 × 40 mm). The data showing the liquidus temperature (LT) and the low eutectic temperature (LET) is shown in Figure 1.

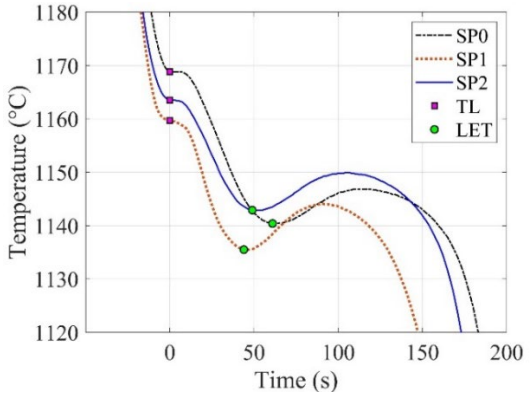

Figure 1. Cooling curves of the three samples showing the liquidus temperature (TL) and the low eutectic temperature (LET). The data was shifted in order to have TL for all samples starting from zero.

Table 3 shows the thermal analysis parameters recalescence (R) and solidus temperature (TS), alongside with liquidus temperature (TL) and lower eutectic temperature (LET).

Table 3. Thermal Analysis Parameters

Sample	TL	LET	R	TS
SP0	1169°C (2136°F)	1140°C (2085°F)	6°C (11°F)	1094°C (2001°F)
SP1	1160°C (2119°F)	1136°C (2076°F)	9°C (15°F)	1082°C (1979°F)
SP2	1164°C (2126°F)	1143°C (2089°C)	7°C (13°F)	1092°C (2005°F)

Note that the TL values follow C wt% in Table 2, showing that the sample SP0 has the lowest C content, while SP1 has the highest, which is due to the carbon addition in the holding furnace. The highest nucleated sample, quantified by LET, is SP2, followed by SP0, while the lowest is SP1. These results are in contradiction with literature data,[2,7] that often reports the reason for the low nucleation level in extended holding time irons is due to carbon loss.

MICROSTRUCTURE

Figure 2 shows the microstructure of the three collected samples. Samples SP0 and SP1 have substantial amounts of undercooled graphite, which is in line with the TA curves shown in Figure 1. Sample SP1 has the lowest nucleated condition, even after the carbon addition. Sample SP2 has clearly the highest nucleation level and far more type A graphite than SP0 and SP1. This modification could be due to the addition of freshly melted raw materials, such as pig iron, SiC, recarburisers, and ferrosilicon additions, which can contain Ca.[6]

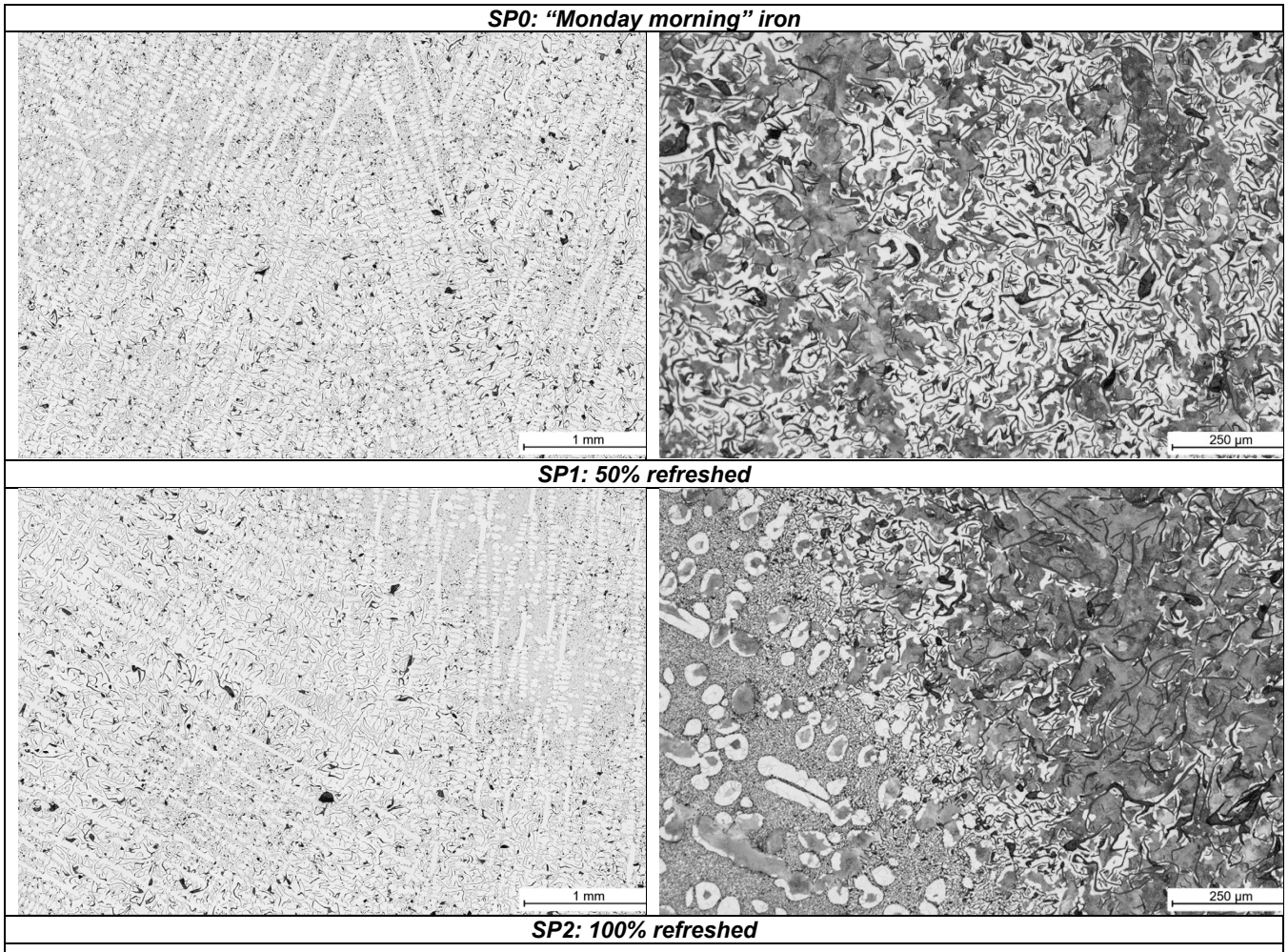

Figure 2. Microstructures of the base iron bases. Top row: SP0, the "Monday morning" iron, Middle: SP1, same melt but with refreshment of carbon. Bottom view below.

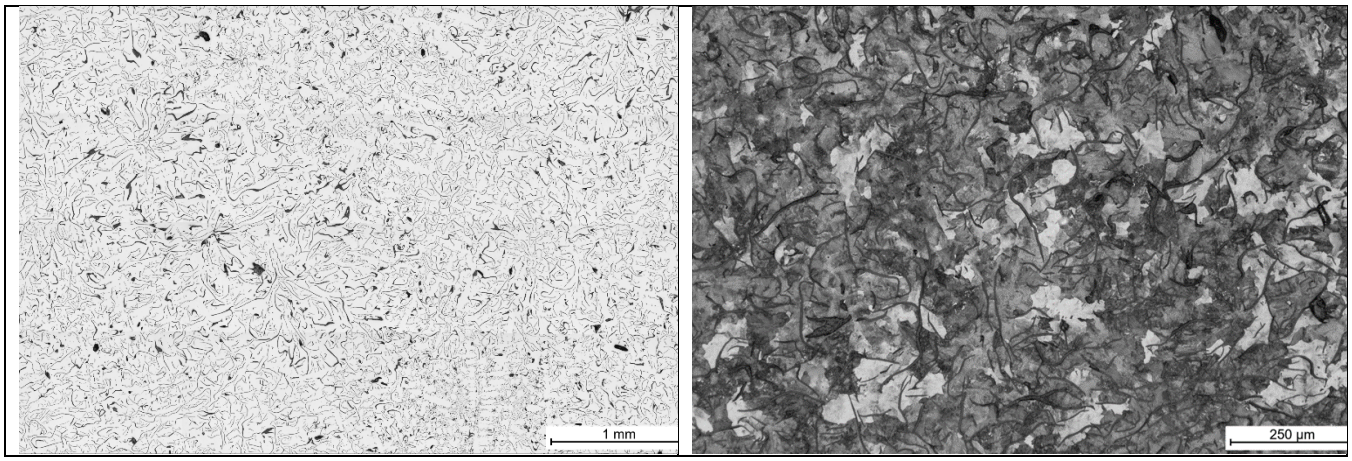

Figure 2. cont'd. Microstructures of the base iron bases. Top row: SP0, the "Monday morning" iron & Middle row: SP1, same melt but with refreshment of carbon (on previous page). Bottom view (this page): melt with new raw materials ready for production.

AMICS

To understand the reasons for the different microstructures and nucleation levels, all the samples were scanned using scanning electron microscopy/energy dispersive X-ray (SEM/EDX) analysis as explained previously. The microinclusions are divided into categories shown in Table 4. Figure 3 shows a typical AMICS treated image.

Table 4. Microinclusions Categories

Category	Elements	Example of spectra
Oxides	Al-Mg-O Al-O	Too small to be detected
Sulfides	Mn-S	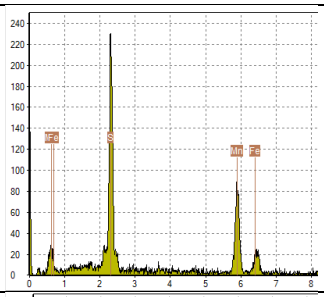
Carbides	Ti-Nb-C	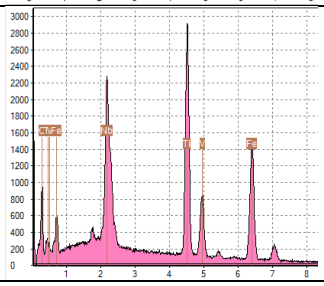

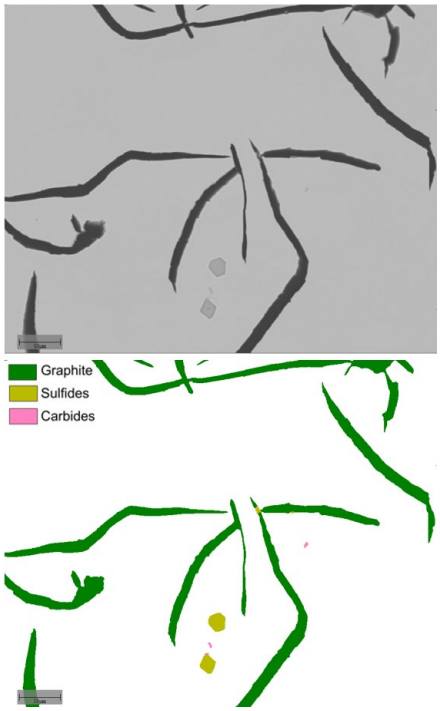

Figure 3. Typical images of an AMICS treated sample. Top: backscattering image, Bottom: segmented image with categories described in Table 4.

The number densities and area fraction for each inclusion category is shown in Figure 4.

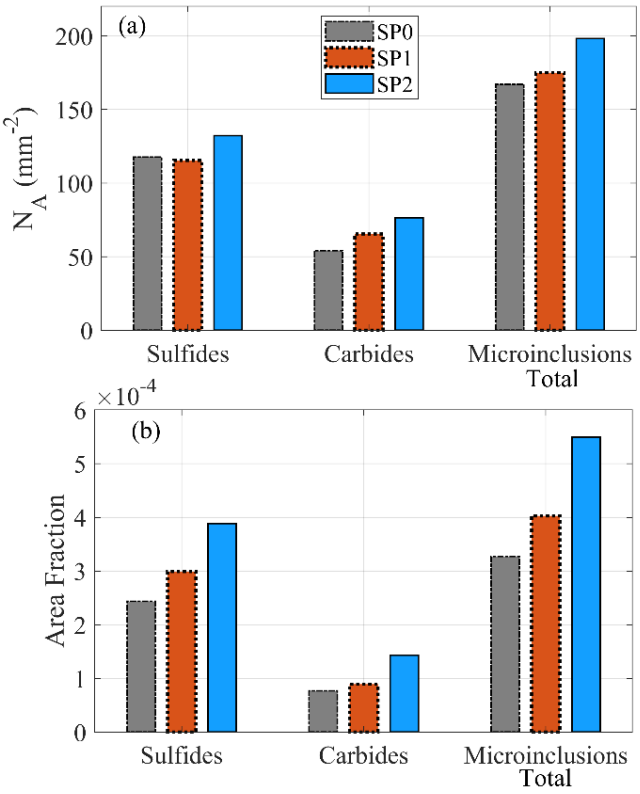

Figure 4. (Top) Number density and area fraction (Bottom) of sulfides, carbides and with the total amount of microinclusions.

Sulfides and carbides are the main detected microinclusions in all samples as seen in Figure 4 (top). Oxides, although present, are too few and too small (below the 0.5 μm^2 size threshold). But when detected they are mainly Al-Mg-oxides, as reported previously.[10,11] The sulfides are all MnS, but their attachment to carbides or oxides can give several different EDX spectra. These sulfides are the predominant particles in the system, and there is not substantial difference between their number density in the samples. A trend can be observed by the density of carbides, with SP1 and SP2 have more than SP0, which could be due to the carbon addition. In general, SP2 has more microinclusions than the other samples.

In the area fraction, shown in Figure 4 (bottom), the fraction of sulfides, carbides, and consequently the total microinclusions in SP2 is substantially higher than the other samples. But note that there is no difference in the S levels in Table 2, which implies that an element present in the raw materials may have promoted the formation of more sulfides.

The difference in the nucleation level of the melt could be related to the shape of these microinclusions. Figure 5 shows the shape of the MnS sulfides measured in all samples. Note that sample SP0 and SP1 contains more "needle-like" particles, while in SP2 they are mostly compacted or rounder. Some of the particles contain a white spot on the middle, which points to another phase in the center; which in most cases are found to be (Al-Mg-oxides)

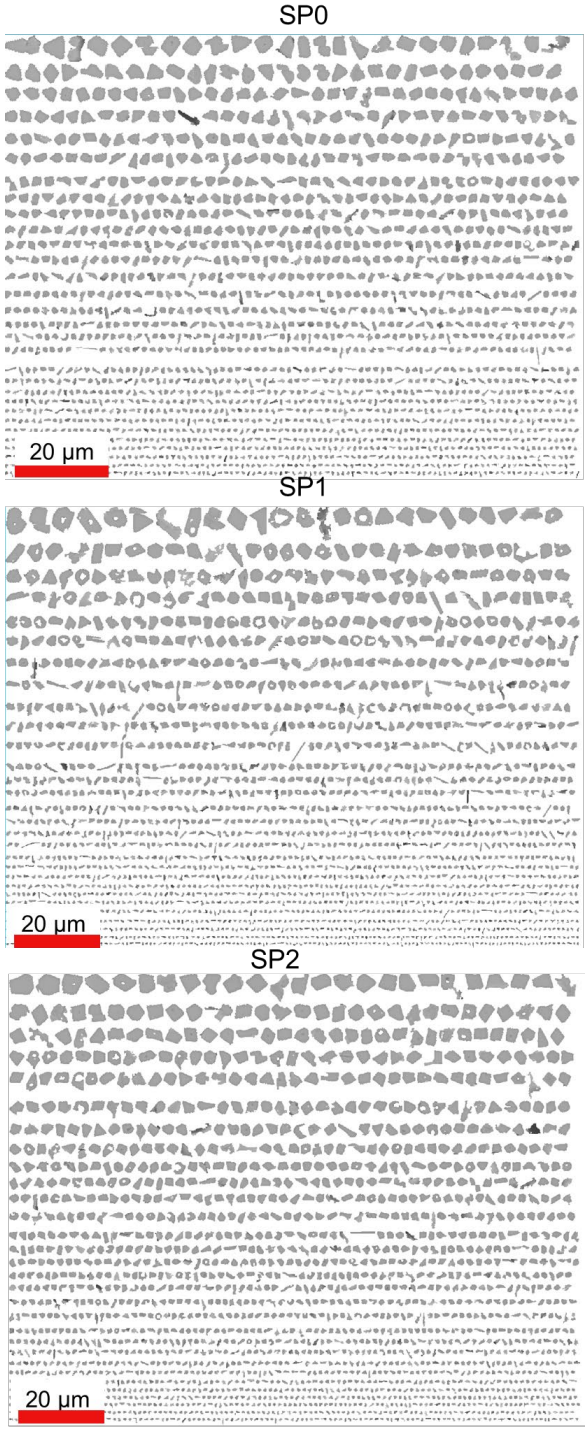

Figure 5. The sulfides measured in all samples sorted by size.

Similarly, the morphology of carbides can be seen in Figure 6. The carbides are (Ti, Nb)C, and have several different shapes, but some appear to be compacted, while others are more elongated.

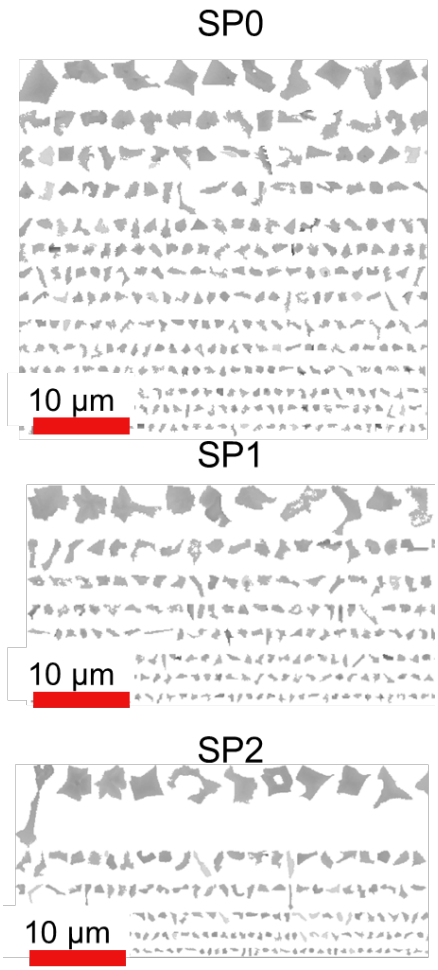

Figure 6. The carbides measured in all samples sorted by size.

The Ti-containing carbides are often observed in grey iron, however the role of these particles in the nucleation is questionable.[11,12] They are a result of carbon absorption from the melt forming recognizable cuboid particles, as seen in Figure 6. There is not a noticeable difference in carbides from different samples, only that SP2 has a slightly higher fraction.

DISCUSSION

As stated in the Introduction, there are mainly three reported reasons for the lower graphite nucleation in a cast iron melt: the carbon loss, coarsening of microinclusions (Ostwald ripening), and loss of microinclusions.

In the case of carbon loss, the argument is that either a nucleation level decreases with a lower carbon equivalent or the assumption that extended holding time of the melt causes the dissolution of undissolved graphite.[6] The present results contradict both. As seen in Figure 1 and Table 2, SP0 is the sample collected from a "Monday morning" melt, it contains lower carbon than the other samples, which is clear from the higher TL temperature. However, the addition of extra carbon in the melt (SP1) did not increase the nucleation level, to the contrary, as it has an even lower LET and poorer microstructure, as seen in Figures 1 and 2. Therefore, loss of carbon cannot explain the lower nucleation level of SP0 and SP1.

For the loss and coarsening of microinclusions, Figure 7 shows the size distribution of all microinclusions in the samples.

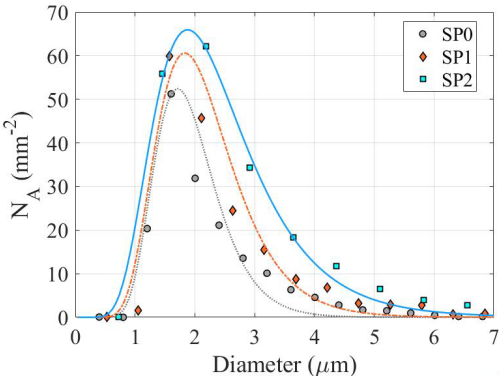

Figure 7. Size distribution of the microinclusions in each sample.

Indeed, the Monday morning iron sample SP0, has a lower amount of microinclusions, as seen in both Figure 7 (and Figure 4). However, they are not coarser. The graphite addition in the sample SP1 showed an increase in the number and slightly coarsening in the microinclusions, while SP2 has the largest area and distribution width of all samples. Therefore, microinclusions coarsening is not the case for poor nucleation, and if loss of inclusions were, then SP1 should not have the lowest LET (Figure 1) and poorest microstructure (Figure 2). Similar observations were made in the study of holding time effect in Mg-treated irons and inoculated irons,[5] it was reported a lower LET as a function of time, but no loss of microinclusions.

Another possibility for a poorer nucleation level, in the case of grey iron, could be the shape of the microinclusions, especially sulfides. The morphology of these particles can be quantified based on their roundness. Figure 8 shows the roundness for both sulfides and carbides.

The roundness (R) is defined in Eqn. 1 as:

$$R = \frac{4A}{\pi d_f^2} \qquad \textbf{Eqn. 1}$$

Where: A and d_f are the area and major axis of the microinclusion. The inverse of R, in Equation (1) is also defined as the aspect ratio. For a perfect circle, $R = 1$. Most sulfides in all samples have a roundness of around 0.8. However, SP2 has more sulfides with a roundness on that value than the other samples. The sample with less rounder sulfides is SP1, which is the sample with the poorest microstructure, and contains the highest carbon. The carbides have a roundness between 0.5 and 0.7.

The relationship between sulfides and graphite morphology in grey iron has been studied by Riposan et al.[9,10] The authors concluded that the addition of trace elements, particularly Ca and Sr can significantly modify the shape of the sulfides. When these elements are present the MnS becomes rounder, and this has been associated with type-A graphite structure. Since SP2 has a substantially improved microstructure, it is implied that the fresh melt could contain Ca, since Sr is mostly found in inoculated grey iron. This element can be present in pig iron and ferrosilicon, causing an improvement in the melt's nucleation condition. However, it is also known that Ca has a fast fading effect. It has been reported that its effectiveness is reduced by approximately 40% in less than 10 minutes.[5,13]

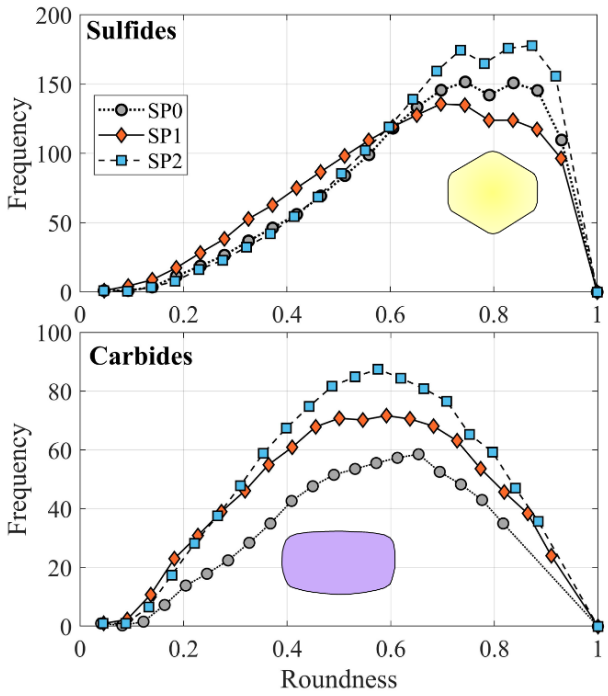

Figure 8. The roundness distribution of sulfides and carbides in each sample. In the inset of each graph a geometrical figure with roundness 0.8 (top) and 0.5 (bottom) is shown.

CONCLUSION

The present work investigated the characteristics of "Monday morning" iron, which is a melt that was held for an extended period, the effect of carbon addition, and the difference from a melt that is ready for production.

The carbon loss cannot explain the low nucleation level of the iron, since the sample that had a carbon addition had the highest undercooling (lowest low eutectic temperature) and a poor microstructure. However, the "Monday morning" iron sample contained fewer finer microinclusions, which was opposite the coarsening predicted in the literature.

The results indicated that the main cause for the low nucleation of the melt was the morphology of the manganese sulfides, MnS. The sample ready for production contained more sulfides with higher roundness than in the "Monday morning" iron.

ACKNOWLEDGMENTS

The authors would like to thank Antônio Carrascosa Filho, Emmanuelle Ott, and Gro Eide from Elkem Silicon Products for their support. Finally, the authors thank Henny Hartung for facilitating the technical discussions.

REFERENCES

1. M. Chisamera, I. Riposan, S. Stan, D. White, G. Grasmo, Graphite nucleation control in grey cast iron, *Int. J. Cast Met. Res.* 21(1-4) (2008) 39-44.
2. J. Campbell, A hypothesis for cast iron microstructures, *Metall. Mater. Trans. B* 40 (2009) 786-801.
3. I. Riposan, T. Skaland, Modification and inoculation of cast iron, Cast Iron Science and Technology Handbook; Stefanescu, DM, Ed.; American Society of Materials: Cleveland, OH, USA (2017) 160-176.
4. L. Michels, B. Cygan, M. Pawlyta, J. Jezierski, A. Götz, J. Akola, Graphite nucleation on (Al, Si, Mg)-nitrides: Elucidating the chemical interactions and turbostratic structures in spheroidal graphite cast irons, *Carbon* (2024) 118848.
5. L. Michels, A.J.F. Pires, C.A.S. Ribeiro, B. Kroka, E.G. Hoel, E. Ott, C. Hartung, Effect of Holding Time on Populations of Microparticles in Spheroidal Graphite Irons, *Metall. Mater. Trans. B* 53(2) (2022) 836-847.
6. E. Fraś, H. López, Eutectic cells and nodule count—an index of molten iron quality, *Int. J. Metal. Cast.* 4 (2010) 35-61.
7. M. Popescu, J. Thomson, R. Zavadil, M. Sahoo, Summary of AFS Research Project on Restoring Techniques for Monday Morning Iron-Phase I, *Transactions of the American Foundry Society* and the One Hundred Sixth Annual Casting Congress, 2002, pp. 1047-1065.
8. T. Skaland, Ø. Grong, T. Grong, A model for the graphite formation in Ductile Cast Iron: Part I. Inoculation Mechanisms, *Metall. Trans. A* 24(10) (1993) 2321-2345.
9. I. Riposan, M. Chisamera, S. Stan, T. Skaland, Graphite nucleant (microinclusion) characterization in Ca/Sr inoculated grey irons, *Int. J. Cast Met. Res.* 16(1-3) (2003) 105-111.
10. I. Riposan, M. Chisamera, S. Stan, C. Hartung, D. White, Three-stage model for nucleation of graphite in grey cast iron, *Mater. Sci. Technol.* 26(12) (2010) 1439-1447.
11. A. Sommerfeld, B. Tonn, Theory of graphite nucleation in lamellar graphite cast iron, *Int. J. Metal. Cast.* 3 (2009) 39-47.
12. E. Moumeni, D.M. Stefanescu, N.S. Tiedje, P. Larrañaga, J.H. Hattel, Investigation on the effect of sulfur and titanium on the microstructure of lamellar graphite iron, *Metall. Mater. Trans. A* 44(11) (2013) 5134-5146.
13. E. Fras, M. Górny, Fading of inoculation effects in ductile iron, Archives of Foundry Engineering 8(1) (2008) 2008.